Nat. Hazards Earth Syst. Sci. Discuss., 1, 747–791, 2013
www.nat-hazards-earth-syst-sci-discuss.net/1/747/2013/
doi:10.5194/nhessd-1-747-2013

Natural Hazards and Earth System Sciences
Open Access
Discussions

This discussion paper is/has been under review for the journal Natural Hazards and Earth System Sciences (NHESS). Please refer to the corresponding final paper in NHESS if available.

Shallow landslides stochastic risk modelling based on the precipitation event of August 2005 in Switzerland: results and implications

P. Nicolet[1], L. Foresti[1,2], O. Caspar[1], and M. Jaboyedoff[1]

[1]Center of Research on Terrestrial Environment, University of Lausanne, Lausanne, Switzerland
[2]Centre for Australian Weather and Climate Research, Bureau of Meteorology, Melbourne, Australia

Received: 28 February 2013 – Accepted: 12 March 2013 – Published: 28 March 2013

Correspondence to: P. Nicolet (pierrick.nicolet@unil.ch)

Published by Copernicus Publications on behalf of the European Geosciences Union.

Abstract

Due to their relatively unpredictable characteristics, shallow-landslides represent a risk for human infrastructures. Multiple shallow-landslides can be triggered by large spread precipitation events. The event of August 2005 in Switzerland is used in order to propose a risk model to predict the expected number of landslides based on the precipitation amounts and lithological units. The spatial distribution of rainfall is characterized by blending data coming from operational weather radars and a dense network of rain gauges with an artificial neural network. Lithologies are grouped into four main units, with similar characteristics. Then, from a landslide inventory containing more than 5000 landslides, a probabilistic relation linking the precipitation amount and the lithology to the number of landslides in a 1 km^2 cell, is obtained. In a next step, this relation is used to randomly redistribute the landslides using Monte-Carlo simulations. The probability for a landslide to reach a building is assessed using stochastic geometry and the damage cost is assessed from the estimated mean damage cost using an exponential distribution to account for the variability. Although the outputs reproduce well the number of landslides, the number of affected buildings is not reproduced by the model. This seems to results from the human influence on landslide occurrence. Such a model might be useful to characterize the risk resulting from shallow-landslides and its variability.

1 Introduction

Shallow landslides often represent a risk for housing, people and infrastructures. Compared with deep-seated landslides, shallow landslides usually trigger spontaneously, flow at higher speed and are not likely to affect repeatedly the same location due to the changes in soil stability conditions (e.g. van Westen et al., 2006; Corominas and Moya, 2008). Consequently, most research efforts focus on the prediction of their exact location and, less frequently, their timing. Several methods for the mapping of landslide susceptibility exist and are based on physical models (e.g. Pack et al., 1998; Montgomery and Dietrich, 1994; Godt et al., 2008) or statistical approaches (e.g. Carrara et al., 1991). Since rainfall has been recognized as being a frequent triggering mechanism (e.g. Wieczorek, 1996), many authors, following Campbell (1975) and Caine (1980), proposed early-warning systems based upon criteria of precipitation intensity and duration (e.g. Guzzetti et al., 2008). Other studies also use the antecedent precipitation as a proxy for considering the groundwater level preceding the precipitation event (Crozier, 1999; Glade et al., 2000). More direct approaches are based upon the real-time monitoring of soil moisture (Matsushi and Matsukura, 2007; Baum and Godt, 2010) or the use of transfer functions to estimate the soil water content from precipitation measurements (Cascini and Versace, 1988; Capparelli and Versace, 2011; Greco et al., 2013).

Many rainfall-induced large landslide events have been recognized worldwide, for example in Italy (Crosta, 1998; Crosta and Frattini, 2003; Crosta and Dal Negro, 2003; Cardinali et al., 2006; Gullà et al., 2008), Spain (Corominas and Moya, 1999), USA (Campbell, 1975; Whittaker and McShane, 2012), New Zealand (Crozier et al., 1980; Glade, 1998; Crozier, 2005), Taiwan (Yu et al., 2006), the Portuguese island of Madeira (Nguyen et al., 2013) and in Switzerland (Bollinger et al., 2000).

Despite the numerous contributions to the physical understanding of the phenomenon itself (for a broad reference list, although not up to date, see De Vita et al., 1998), studies on the assessment of landslide risk are less commonly found in the literature. Examples of quantitative risk analysis (QRA) at regional scale can be found in Cardinali et al. (2002), Remondo et al. (2005) or Catani et al. (2005). However, these studies provide a mean annual risk with no information on the expected distribution of annual costs. More recently, applications of regional scale QRA providing exceedance probabilities were presented in Jaiswal et al. (2011) and Ghosh et al. (2012). Although, most of the QRA methodologies are developed for local or regional scales, some of them, as for example Catani et al. (2005), might be applied to a larger area.

Switzerland was affected in August 2005 by a rainfall event with measured precipitation reaching 324 mm in 6 days. Although floods were the main damage cause, more than 5000 landslides were reported (Raetzo and Rickli, 2007). Landslide-induced damage has been estimated by Hilker et al. (2007) at 92 million Swiss francs (USD 99 million; debris-flows not included) and represents 4.5 % of the total damage cost.

As already mentioned by Jaboyedoff and Bonnard (2007) and by Rickli et al. (2008), landslide density was highly correlated with the total precipitation amount. Following their ideas, this article proposes a risk model for shallow landslides based on the event of August 2005. The input parameters of the model include a rainfall and a lithological map. The map of 6 day rainfall accumulations is constructed by interpolating a high resolution rain gauge network using weather radar data as external drift. A geotechnical map is interpreted in order to group different units into 4 main lithological settings. The expected number of landslides is predicted as a function of rainfall level conditional to the lithological type. An intersection probability concept is then employed to predict the potential number of landslides affecting buildings and the corresponding damage cost.

The paper is structured as follows. Section 2 details the rainfall event of August 2005 in Switzerland both from a meteorological and lithological viewpoint. Section 3 explains the methodology to assess the landslide probability as a function of rainfall accumulation and lithological context. Section 4 presents the risk analysis results in terms of expected number of landslides, number of affected buildings and associated cost. Finally, Sects. 5 and 6 discuss and conclude the paper.

2 The rainfall event of August 2005 in Switzerland

2.1 Study area

The study area covers the entire Swiss territory (around 42 000 km^2), which extends from the Jura mountains in the North-West, to the Alps, in the South-East, through the Molassic Plateau, where most of the population is concentrated. Special attention is

Discussion Paper | Discussion Paper | Discussion Paper | Discussion Paper |

given to the location where most of the landslides occurred, which is the central part of Switzerland, between the cities of Bern and Lucerne (Fig. 1). Landslides occurred in the tectonic units described below (Trümpy, 1980; University of Bern and FOWG, 2005a,b), which are listed along a northwest-southeast direction (perpendicularly to the geological structures):

- Upper Freshwater Molasse from Middle and early Upper Miocene (consisting of floodplains sediments including puddings, sandstones and silty shales).
- Other types of Molasse (narrower areas of Upper Marine Molasse, Lower Freshwater Molasse and Lower Marine Molasse, the lower part of this series being in Subalpine position).
- Subalpine Flysch.
- Upper Penninic Flysch (Schlieren Flysch).
- Ultrahelvetic and Helvetic Nappes (including tertiary shallow marine formation and Cretaceous Limestones from the Wildhorn nappe and Jurassic Limestones from the Axen nappe).

Soils (regolith) and loose materials cover most of the time the bedrock. Most of these shallow and superficial formations have not been mapped, except for the cases where the formation reaches a sufficient extension or thickness to be considered relevant at the map scale. This is for example the case of morainic material deposited by the glaciations during the Quaternary, which is visible at several places, especially on the Plateau (Trümpy, 1980). The properties of the local soils strongly depend on the underlying bedrock.

2.2 Description of the precipitation event

The rainfall event of August 2005 in central and eastern Switzerland resulted in severe damage due to flooding and induced slope instabilities (Rotach et al., 2006). The

presence of the Alps played a key role in controlling the spatial distribution of rainfall due to orographic precipitation enhancement processes. Persistent precipitation patterns were mostly found on the exposed upwind slopes under northerly and northeasterly flow conditions as studied by Foresti and Pozdnoukhov (2011) and Foresti et al. (2012). In particular, the stratiform precipitation was locally enhanced by smaller scale orographic features leading to persistent initiation and enhancement of the embedded convection.

The most intense period of the event was observed between 21 and 22 August. Driven by cyclonic conditions during the first day, the moist air from the Mediterranean sea circumvented the Austrian Alps and started approaching slightly crosswise the northern slopes of the Swiss Alps from the east. The mesoscale flows gradually turned from easterly to northerly conditions during the second day. The reduced supply of air moisture was compensated by a stronger upslope rainfall enhancement which extended the duration of precipitation. The return period for 48 h rainfall accumulations largely exceeded 100 yr at several weather stations mostly located in the Berner Oberland (Rotach et al., 2006). It is worth mentioning that the uncertainty of this estimation is quite important as an event of such intensity was never observed in the past at the considered weather stations.

2.3 Landslide inventory

As a consequence of this extreme rainfall event, many shallow landslides were triggered, mainly in the Entlebuch part of Lucerne canton and in the Bern canton. Some deep-seated landslides were observed as well and are mainly located farther southeast. A landslide inventory has been collected by Raetzo and Rickli (2007) from cantonal authorities information and contains 5756 landslides (Fig. 1). Although some additional attributes such as the exact timing have been registered for some of the landslides, we only dispose of the version provided in the above publication and, as a result, we only know the approximate location. The uncertainty about the location of landslides complicates the analysis of geological context.

Statistics on the landslides can be found in Raetzo and Rickli (2007) and in Rickli et al. (2008) and investigations on specific sites in Mueller and Loew (2009) and von Ruette et al. (2011). The travel distance of shallow landslides has been analyzed for 148 cases and ranges from a few meters up to 500 m (Raetzo and Rickli, 2007). Around 75 % of the landslides traveled less than 100 m and 90 % less than 200 m (Fig. 2).

2.4 Damage

According to the Swiss Federal Institute for Forest, Snow and Landscape Research WSL, the 2005 event has been the most costly since the beginning of the collection of damage data in 1972, with a total damage cost estimated at 1.87 billion swiss francs (around USD 2 billion). On the other hand, in spite of being the most important event recorded, other years have been equally or more damaging regarding landslides in the past 40 yr (Hilker et al., 2009; WSL, 2012).

Hilker et al. (2009) divided the damage values into three categories according to the cause, namely floods, debris flows and landslides (including mud-flows). Landslides represent around 4.5 % of the total cost and affected private properties (22 %, CHF 16.3 million) and public infrastructures (88 %, CHF 75.6 million) (Hilker et al., 2007). Private damage includes damage to buildings as well as furnitures, vehicles, other property damage and loss of profits. Comparatively, public damage includes damage to waterways, roads (except small ones), rail, farming and forests. In addition to economic consequences, six casualties are to be deplored.

3 Risk modeling methodology

3.1 Introduction

The annual risk to property is usually evaluated with the following equation (Dai et al., 2002; Fell et al., 2005):

$$R(PD) = P(L) \times P(S|L) \times V(P|S) \times E \tag{1}$$

where L denotes the landslide, P the element at risk (property) and S the impact. $P(L)$ represents the landslide frequency, $P(S|L)$ the spatial probability of the landslide reaching the element at risk, $V(P|S)$ the vulnerability of the element at risk to the landslide impact and E the element at risk value.

In the case studies considered in this article, this equation is not used directly since a single precipitation event is used as an input. However, since this event is used to redistribute the landslides according to the precipitation event, $P(L)$ is not completely left out. In a first phase, the spatial distribution of the event rainfall accumulation is estimated using data from a dense network of rain gauges and addional C-band weather radars (Sect. 3.2). The second phase studies the statistical distribution of landslides as a function of precipitation intensity and lithological type (Sect. 3.3) and is used to estimate the probability of landsliding $P(L)$. It must be mentioned that $P(L)$ should also account for the climatological frequency, which is the probability of the precipitation event to occur. As the analyses consider only one single event, this probability was set to 1 and the term $P(L)$ is only estimated from the distribution of landslides conditional to the precipitation event. $P(S|L)$ is assessed using principles of stochastic geometry, and represents the probability of buildings to be affected by circular landslides within a given cell. This term partially accounts for $P(L)$ since the exact location of the landslides within the cell is randomly assigned at this step. The separate estimation of the terms $V(P|S)$ and E is not possible as the cost of damages is assessed directly (see Sect. 3.4).

Discussion Paper | Discussion Paper | Discussion Paper | Discussion Paper |

3.2 Spatial analysis of rainfall

MeteoSwiss operates an automatic network of 76 weather stations and a dense network of additional 363 rain gauges. The automatic network measures rainfall with a temporal resolution of 10 min while the second only reports daily accumulations from 05:40 to 05:40 UTC of the next calendar day. An additional network of 3 C-band radars is used to measure precipitation with higher spatial resolution. The operational radar data processing chain for quantitative precipitation estimation (QPE) at MeteoSwiss includes the removal of ground clutter, correction for the vertical profile of reflectivity in connection with the bright band effect, climatological rain gauge adjustment, the interpolation from polar coordinates to a Cartesian grid, and the use of a fixed climatological Z–R relationship (refer to Germann et al., 2006, for more details). A geostatistical method for real-time bias adjustment with rain gauges was only recently implemented by Sideris et al. (2013). For long term evaluation of the radar QPE accuracy against rain gauges refer to Gabella et al. (2005). The radar QPE product used in this paper is a $1\,\text{km}^2 \times 1\,\text{km}^2$ grid of the rainfall accumulation during the period 18–23 August 2005.

Despite these corrections, the product still contains residual ground clutter and biases due to the blockage of low level radar beams, in particular in the inner Alpine valleys. To partially account for these issues, an artificial neural network was applied to blend the radar-based QPE map with the rain gauge rainfall accumulations. A 3-H-1 multiLayer perceptron (MLP) was trained to predict the rainfall amount observed at the rain gauges as a function of 3 variables: the geographical location represented by the Swiss Easting and Northing coordinates and the radar QPE product which acts as an external drift. The geographical coordinates account for the observed biases between rain gauges and radar-based QPE, which show a significant spatial dependence. A conjugate gradient algorithm was employed to train the network. A low number of hidden neurons H was chosen to obtain a smooth representation of the spatial rainfall biases. The optimal model was selected by minimizing the leave-one-out cross-validation root-mean square error (RMSE). A randomly sampled test set was kept to evaluate the

expected prediction RMSE, which is of 25.28 mm. No quantitative assessment of the performance of the MLP model against geostatistical approaches (e.g. Sideris et al., 2013) was carried out. The regularized MLP solution is a smooth compromise between the radar and rain gauge measurements. This allows being robust to local radar overestimations due to ground clutter and the different sampling volume of radar and rain gauge measurements. The Machine Learning Office software was used for the computations (Kanevski et al., 2009).

Figure 3 illustrates the spatial analysis of the rainfall accumulation from 18 to 23 August 2005. The highest accumulations are observed on the northern slope of the Alps, in particular along a line from the Berner Oberland to the mountain range of Saentis. The spatial distribution of landslides closely follows the regions with the highest rainfall totals with some spatial heterogeneity due to the different geological settings.

3.3 Landslide distribution

To be consistent with the precipitation map, the resolution of the landslide distribution maps has also been set to $1\,\text{km}^2 \times 1\,\text{km}^2$. For each grid cell, the probability to exceed a given number of landslides is computed based on the rainfall amount and the lithological type.

Geology is extracted from the 1 : 200 000 geotechnical map of Switzerland (BFS GEOSTAT/BUWAL) and transformed from a vector map to a $m \times n \times p$ cumulative matrix which gives, for each cell, the proportion of each lithological unit (Figs. 4 and 5). The geotechnical types have been simplified into 4 different units, loosely based on the 6 units used by Rickli et al. (2008) to assess the landslide density distribution of the event:

- Limestone Formations (LF),
- Cristalline Formations (CF),
- Flysch, Loose material (except moraine), Marls and Claystones (FLMC),

– Molasse and Moraine (MM).

Cells that contain water (lake or glacier) or that are located on the Swiss border have a cumulative value below 1 (Fig. 4e). The model is run several times and assigns at each iteration a unique lithological unit following the probabilities given in the maps shown in Fig. 4.

Landslides are transformed from point features to a raster displaying the landslide number in each cell (Fig. 1). This raster is then multiplied by the cumulative geological raster (Fig. 4e) to take into account the smaller land surface inside the cell. Indeed, cells with a total value below one for the geology (borders of Switzerland, lakeshores, etc.) are taken into account only at some iterations. Therefore, by dividing them with the geology allows to maintain a mean number of landslide consistent with the inventory.

The precipitation field has been divided into 15 classes based on given quantiles and the statistical distribution is shown in Fig. 6. The histogram is highly skewed and only 10 % of the region exceeds 200 mm of rain.

Figure 7 summarizes the data processing workflow. The output of the model is a cumulative distribution of the landslide number given the geology and the precipitation amount. To allow a generalization of these results, gamma distributions were fitted to the data by minimizing the mean square error in order to model the number of landslides as a function of precipitation amount. Since the gamma distribution is a continuous distribution whose domain is $0 \rightarrow \infty$, it this not exactly suitable to fit discrete data, especially as the highest frequency is obtained at a value of 0 (we can indeed expect that 0 landslides in a cell is always the most frequent, regardless of the precipitation amount). However, this problem has been solved by shifting the cumulative frequencies to the upper number of landslides to fit the distributions, and by rounding down the number of landslides obtained for a given quantile when using the inverse distribution function.

To estimate the models predictive ability, a second part consists in using the distribution previously assessed to simulate different potential consequences of the precipitation event using a Monte-Carlo approach. This step illustrate the uncertainty of the

model on the consequences of a given precipitation event. Indeed, since we consider that the landslides are controlled only by the precipitation and the lithology this step gives the variability resulting from this simplification. The workflow of this step is given in Fig. 8.

3.4 Impact assessment

The impact assessment consists of two main steps, which are evaluating how many buildings will be reached and estimating an associated cost. In order to asses the number of affected buildings, a concept of stochastic geometry is used. Assuming that the landslide has the same probability to occur anywhere within the cell, the conditional probability that any building of the cell is reached if a dimension-less landslide occurs is given by the proportion of the cell covered by buildings. To take into account the landslides dimensions, a buffer is added to the buildings. Indeed, as shown in Fig. 9, if the landslide is considered to be circular, it will affect a house if its center is located inside the buffer area (buildings included). As a result, the conditional probability is calculated considering the surface covered by the houses and their buffers. Since the buffers can overlap, the resulting probability considers the intersection with at least one building. Although landslides are usually not circular but have an elongated shape, a circle is used in order to simplify the model by avoiding the need to consider a real geometry. Indeed, for non-circular landslides, the intersection probability cannot be simply reduced to a single number for each cell, since the intersection does not depend only on the position of the center, but also on the orientation of the considered shape.

Since, for a given surface, an elongated shape is more likely to intersect a building than a round one, the circle diameter is set to 200 m in order to completely include 90 % of the landslide (Fig. 2). This diameter results in an overestimation of the landslide surface, but takes indirectly into account the landslide geometry and provide a slightly pessimistic risk estimation in terms of number of affected buildings. Thus a 100 m buffer has been added to the 1 814 667 buildings extracted from the vectorized landscape model of Switzerland (Vector25, © swisstopo). Then the total surface has been compared with each cell surface to obtain the intersection probability (Fig. 10). It has to be mentioned that intersection is only considered with a boolean approach, which means that a landslide can affect a building or not, but the potential for one landslide to affect several buildings is not considered. It should also be noted that the buffers are made before cutting shapes into cells in order to take into account the possibility for a landslide occurring in a given cell to reach a house located close to the border of an adjacent cell.

The estimation of the associated cost is more complicated as the value of the buildings is not known. This information could be obtained from the buildings insurance for 19 over 26 cantons for which a public insurance exists and is mandatory. However, a suitable vulnerability curve linking the landslide intensity, characterized by parameters such as depth or area, to the damage rate, is difficult to assess. The lack of knowledge on the precise landslide characteristics and location as well as the inherent variability of the elements at risk complicates even more the assessment of the vulnerability (Galli and Guzzetti, 2007). Therefore, in order to keep the models precision consistent with the previous step, we chose not to use a value and vulnerability curve to assess the damage cost, but to assess it directly from the 2005 event mean damage cost.

The expected damage cost for a given building x is assumed to follow an exponential distribution with probability density function:

$$f(x) = \begin{cases} \lambda \exp(-\lambda x), & x \geq 0 \\ 0, & x < 0 \end{cases} \tag{2}$$

The distribution is only defined in terms of its first moment λ, which is equal to $\bar{x}^{-1}$, $\bar{x}$ being the expected mean damage cost per building assumed for the 2005 event. This cost is estimated by dividing the total damage cost induced by landslides to private infrastructures (CHF 16.3 million) by the expected number of affected buildings. The latter is obtained by summing over all grid cells the product between the number of landslides (Fig. 1) and the intersection probability (Fig. 10). This approach results in

2360 affected buildings, implying a mean cost $\bar{x}$ of CHF 6907 per building. No uncertainty is considered on this parameter.

The generation of exponential variates is obtained by sampling from the quantile distribution, which is given by the inverse function of the exponential cumulative distribution as:

$$F^{-1}(u) = x = -\frac{\ln(1-u)}{\lambda} \tag{3}$$

where u is a uniformly distributed random number between 0 and 1. The exponentially distributed damage cost is sampled for each case of impact identified by the model.

The fat-tailed nature of the exponential distribution allows obtaining a more realistic estimate of the damage costs than a normal or triangular distribution and does not need the estimation of the second moment characterizing the variance of the distribution. The latter is a useful feature as the statistical distribution of the damage costs per building is not known in our particular case. The lognormal distribution also has heavy tails and was successfully used to model the cost associated to floods (Merz et al., 2004). However, due to the larger number of degrees of freedom, it is also not suitable for our application.

4 Results

The statistical distribution of landslides as a function of precipitation amount and lithological group is given in Fig. 11. The probability to observe a given number of landslides in a given lithological group is a monotonically increasing function of the precipitation amount. CF show a very little susceptibility to landslides compared to the other groups as evidenced by the low number of observed landslides. With similar precipitation amount, MM formations tend to have a higher probability to contain at least one landslide than FLMC or LF. However this relation is less evident for larger landslide numbers.

Table 1 shows the fitted values of the gamma distribution for the highest five precipitation classes, whereas Fig. 12 display these values graphically. CF were not considered due to the low number of samples. The α parameter (shape), characterizes the central location of the distribution, while the β parameter (inverse scale) characterizes its dispersion. A general increase in both α and β parameters with precipitation amount can be observed, although some values are not following the general linear trend. This is especially the case for α for the classes with precipitation lower than 184 mm for LF and lower than 158 mm for FLMC.

The general increase of both parameters is a desirable property and is in accordance with our prior expectations. In fact, increasing precipitation amounts increase the expected number of landslides (represented by α) and the dispersion of the distribution (represented by β). Higher β values are representative of heavy-tails, which means that the probability of observing a high number of landslides rises with increasing precipitation amount.

The spatial distribution of the number of landslides was computed following the procedure described in Fig. 8 using both the raw data and the gamma fits. However, since gamma distributions have been fitted only for the classes containing enough data samples, raw data have been used instead of gamma distributions when not available. The mean modeled number of landslide with gamma fits is given in Fig. 13 and is very similar to the mean number of landslides modeled with raw data. The spatial pattern is relatively similar to the spatial distribution of rainfall amounts, with two remarkable differences. First, the relation between precipitation amount and number of landslides is not linear, which implies that areas with low precipitation amounts show a null to very low number of landslides. The second difference is due to the sharp geographical transitions between the lithological units, which lead to sharp transitions in the modeled number of landslides. An illustrative example occurs when moving from the MM formations the CF, which strongly reduces the number of landslides (see Fig. 4). These results seems to be in good agreement with the observed distribution landslides (Fig. 1).

To evaluate the ability of the gamma fits to reproduce the raw data, maps for the 95th and 98th quantiles have been modeled, still using a Monte-Carlo simulation to account for the probabilistic aspect of the lithology (Fig. 14). Although the results are relatively similar for the 95th quantile (with slightly lower values for the gamma fit), the 98th quantile shows more differences. Indeed, the gamma fit seems to underestimate the number of landslides observed in the raw data and indicates that the end of the tail of the distribution is not adequately represented.

4.1 Impact assessment

Although the landslide number is reproduced, the expected number of hit buildings is almost never reached in the simulations (Fig. 15). Indeed, the expected number of affected buildings for the event is 2360, whereas the simulations return a mean of around 1860. As a consequence, the damage amount is not reached either since it is derived from the latter. Tests have been made using a 20 m buffer for the houses and the same effect was observed. It is not yet clear why the observed total number of hit buildings is underestimated by the model. One possible reason could be that the landslide localization is highly correlated with the buildings location. To test this hypothesis, we compared the intersection probability of cells within which landslides actually occurs to the intersection probability of cells in which the mean modeled number of landslides (Fig. 13) is above 0.5. Considering only these cells allows to keep the most susceptible cells according to the model. This comparison indicates that the modeled landslides tends to occur in cells with lower intersection probability than the actual landslides. This effect is not clearly visible with a 20 m buffer, but is more obvious with 100 m buffers (Fig. 16).

5 Discussion

The landslide model presented in this paper only considers precipitation amounts and geology as input parameters. However, other variables such as terrain slope, soil thickness and permeability contrast, play a key role in shallow landslide generation. These variables are either hard to measure over a large domain, e.g. the soil thickness, or show spatial variability at scales which are smaller than $1\,km^2 \times 1\,km^2$ resolution, e.g. the terrain slope. Additionally, the uncertainty of the landslide inventory does not allow matching the location of the landslide with such high resolution variables. As a consequence, the $1\,km^2 \times 1\,km^2$ resolution model only gives information about the large scale pre-conditioning factors for landslide generation. Smaller scale features may affect the process of landslide triggering in a significant way. Furthermore, this model is based only on one single event and should be compared with other similar rainfall events. In particular, it should be compared with similar events producing landslides in different geological settings, to validate the aggregation of different lithology into four main units. Indeed, landslides susceptibility might be different in Jura limestones than in Prealpine limestones, for example.

The annual probability to overcome a given total damage cost could be assessed by analyzing different precipitation events, which are weighted based on their frequence of occurrence (return period). This step is essential in order to obtain a mean annual cost as well as an exceedance probability curve. One possibility to generate a large number of rainfall fields to appropriately represent the full risk estimation could be based on design storms (Seed et al., 1999). Stochastic rainfall fields could be generated according to a given return period and be used to simulate the spatial distribution of landslides under extreme rainfall conditions. Attempts have been made to use a return period in order to predict landslide triggering but, they were mainly performed at local scale (e.g. Iida, 1999; D'Odorico et al., 2005; Iida, 2004; Tarolli et al., 2011) and would therefore not be suitable for a larger area, since the spatial variability is not taken into account. On the other hand, the spatial distribution of rainfall by means of radar data has been

used for early-warning (e.g. Apip et al., 2010), but as far as we know, is has not been used as in starting point to simulate potential future events.

Another issue concerns the landslide timing. We used the precipitation amount of the whole event (6 days) as a predictor for landslide occurrence. But, shallow-landslides are known to be sensitive to the intensity and duration of the rainfall, as well as to the hyetograph shape (D'Odorico et al., 2005). There are two main reasons for this simplification. The first is the lack of data on the exact timing of landslides, which does not allow analyzing the temporal precipitation pattern preceding their triggering. The second reason is due to the uncertainty of the radar QPE product, which is higher when used to analyze rainfall time series at high temporal resolutions, for instance hourly or 10 min accumulations. The spatial distribution of QPE accuracy can still be affected by some residual ground clutter, which overestimates the true rainfall amount, and by the blockage of low level beams, which leads to the underestimation of ground rainfall due to using only the beams aloft. Wüest et al. (2010) present a method to obtain hourly precipitation fields by disaggregating the daily rain gauge measurements with higher resolution radar fields. If the timing of landslide occurrence was known, this dataset would be a valuable source of information. However, the product is not accompanied by uncertainty estimates. A possible solution could involve the generation of stochastic ensembles to represent the uncertainty of the radar QPE product with respect to the automatic network of 76 meteorological stations. This approach was recently implemented at MeteoSwiss (Germann et al., 2009) and could be a smart alternative to integrate ensembles of precipitation fields together with ensembles of lithological types into the landslide model.

When it comes to the damage cost assessment, due to the lack of information on the number of affected buildings and corresponding distribution of costs, a few important assumptions were made. The total number of affected buildings was estimated by means of an intersection probability and this number was used to obtain a mean cost per hit building. The number of hit buildings is an uncertain estimation since it depends on the exact location of the landslides inside the cell. Indeed, we consider the landslides to be uniformly distributed within a grid cell. This assumption is realistic at the model scale since every $1\,km^2 \times 1\,km^2$ cell contains slopes that might fail. However, if susceptible slopes were located, inside of a cell, far from the houses, the modeled intersection probability would not be null, although it might be the case in reality. We plan to overcome this issue in the future by using a susceptibility map to constrain the landslides location at the intersection probability step.

The distribution of costs was assumed to be exponential, which has a desirable long-tail property and is completely defined by its mean value. Despite being only defined in terms of the average costs, the obtained variability is supposed to adequately represent the reality. Nevertheless, with a mean cost of CHF 6907 per building, the probability to overcome CHF 500 000 is 5×10^{-36}, i.e. one case over 1.8×10^{35}. Since the mean price of a building is around CHF 1 million, this value is quite low as we know that at least one – but probably more – building has been destroyed. This could be the result of a too high number of affected buildings (since they have been estimated), which reduces the mean damage cost, or an indication of the need for using a distribution of damages with a fatter tail. However, this confirms the fact that a distribution with a fat tail is suitable. Nevertheless, since the damage cost varies independently for each affected house and since the number of affected houses is relatively high in the simulations, the effect of these parameters variability is attenuated when summing over all the damage costs. Another problem concerns the absence of data about the type of damage. Therefore, we assumed that all of the private costs are related to buildings. This simplification is not an issue as long as the cost is related to objects located close to or inside the buildings (furnitures, parked cars), but is more problematic for costs related to loss of profits for example. However, we suppose that the vast majority is related to buildings. As a result, this model could be improved considerably if the type of damage was known. Thus, the damage assessment part has to be considered more as an example than as a reference for further vulnerability assessment.

Regarding the number of landslides, hit buildings and the amount of damage in each simulation, the variability of the results follows more or less a normal distribution

(Fig. 15). This distribution reflects the uncertainty induced by the lack of knowledge in the assessment of the consequences of a given precipitation event. Since the model is based on the observed landslides to redistribute the landslides and assess the consequences, the number of modeled landslides using raw data is logically centered around the observed value. Gamma fits results tend, on the other hand, to be lower than using raw data. This is due, in all likelihood, to the lack of ability of the gamma fits to reproduce the high observed numbers of landslides in some single cells. When it comes to the number of hit buildings, the expected value is hardly ever reproduced. Since the same concept of intersection probability, with the same buffer value, is used to assess the expected number of hit buildings of the 2005 event and of the simulation results, this should not be observed. Tests with a 20 m buffer gave similar results. By comparing the intersection probability of the cells in which landslides occurred with those of the cells in which the landslides were modeled, we can observe that the cells in which landslides occurred have higher intersection probability. Different hypotheses can be made in order to explain this effect. First, we might have neglected an important parameter for the localization of landslides which would be correlated to the built areas, redistributing then the landslides in less populated areas. A second option could be related to the quality of the inventory, which would be more complete in urbanized areas. Correcting this effect would imply a greater total number of landslides, with more landslides on area with low intersection probability. The third one, which seems to us the most probable, would be that the urbanization tends to increase the susceptibility. Indeed, human activities can contribute to landslides, acting directly as a trigger or indirectly by destabilizing the slope, according to the classification of Michoud et al. (2011). Since, the trigger of the 2005 event is undeniably the rain, only the latter case can have played a role. Examples of landslides triggered by rain events on slopes destabilized by the modification of pore pressure induced by pipe leaks have been observed in Switzerland, in Les Diablerets (Jaboyedoff and Bonnard, 2007) and in Lutzenberg (Valley et al., 2004). This second example is especially interesting since the landslide occurred within an event involving hundreds of landslides and debris-flows, and since this particular landslide would not have occurred, thanks to the authors, without the pipe leak. Besides modifying pore pressure, pipe leaks can also destabilize slopes by weakening clay minerals (Preuth et al., 2010). In addition, the degradation of old canalization network led to a landslide in 1930 in La Fouvrière hill in Lyon (France), killing 39 persons (Allix, 1930; Albenque, 1931). It would therefore be wise to include a parameter linked to the buildings to take account of this effect.

All things considered, the model makes simplifications in order to assess risk for a large area rather than to be precise at local scale. Indeed, the lack of knowledge and data at the sub-grid scale is balanced by the use of stochastic simulations, which allows obtaining a probabilistic model for landslide occurrence and associated cost.

Such kind of model might be useful to provide a rapid damage estimation following a precipitation event. Indeed, after a widespread event, the time needed by the insurance to process all claims is rather long and consequences might need several months, even years to be known. Applying this model quickly after the event could provide a rough estimation of the damage costs. In a second step, modeling precipitation events assigned to a frequency would make possible the calculation of exceedance probability curves.

6 Conclusions

This article proposes a model to asses risk due to shallow landslides for a large region using the data from 2005 event in Switzerland. Distribution of landslides with regard to precipitation and lithology is assessed in a first step, then the landslides are redistributed according to the relation obtained. Damage cost is obtained by the mean of an intersection probability, which gives the probability, if a landslide occurs, that it reaches a building.

Some improvements have to be made to the model, to corroborate the relation obtained, and to improve the assessment of the intersection probability, as well as the distribution of costs. Moreover, the human influence on landslide susceptibility has to

be evaluate carefully in a further step, since it appears that the landslides locations are highly correlated with the buildings. This observation tends to indicate that the human influence on slope stability is substantial. Further developments are also conceivable to complete the risk analysis by simulating stochastic rainfall events characterized by a frequency and to analyze the consequences. This would result in a complete risk analysis able to provide the temporal distribution of damage costs.

Acknowledgements. This study was partially supported by the Canton of Vaud Natural Hazard Unit and by the the Swiss National Science Foundation project *Data mining for precipitation nowcasting (PBLAP2-127713/1).* We thank the Federal Office of Meteorology and Climatology for providing the data for the rainfall event of August 2005.

References

Albenque, A.: L'éboulement de Lyon, Ann. Geogr., 40, 105–106, 1931 (in French). 767

Allix, A.: L'éboulement de Fourvière (note préliminaire), Les Études rhodaniennes, 6, 454–455, 1930 (in French). 767

Apip, Takara, K., Yamashiki, Y., Sassa, K., Ibrahim, A., and Fukuoka, H.: A distributed hydrological–geotechnical model using satellite-derived rainfall estimates for shallow landslide prediction system at a catchment scale, Landslides, 7, 237–258, doi:10.1007/s10346-010-0214-z, 2010. 764

Baum, R. and Godt, J.: Early warning of rainfall-induced shallow landslides and debris flows in the USA, Landslides, 7, 259–272, doi:10.1007/s10346-009-0177-0, 2010. 749

Bollinger, D., Hegg, C., Keusen, H., and Lateltin, O.: Ursachenanalyse der Hanginstabilitäten 1999, Bulletin für angewandte Geologie, 5, 5–38, 2000 (in German). 749

Caine, N.: The rainfall intensity – duration control of shallow landslides and debris flows, Geogr. Ann. A, 62, 23–27, 1980. 749

Campbell, R. H.: Soil Slips, Debris Flows, and Rainstorms in the Santa Monica Mountains and Vicinity, Southern California, Professional paper 851, US Geological Survey, Washington, 1975. 749

Capparelli, G. and Versace, P.: FLaIR and SUSHI: two mathematical models for early warning of landslides induced by rainfall, Landslides, 8, 67–79, doi:10.1007/s10346-010-0228-6, 2011. 749

Cardinali, M., Reichenbach, P., Guzzetti, F., Ardizzone, F., Antonini, G., Galli, M., Cacciano, M., Castellani, M., and Salvati, P.: A geomorphological approach to the estimation of landslide hazards and risks in Umbria, Central Italy, Nat. Hazards Earth Syst. Sci., 2, 57–72, doi:10.5194/nhess-2-57-2002, 2002. 749

Cardinali, M., Galli, M., Guzzetti, F., Ardizzone, F., Reichenbach, P., and Bartoccini, P.: Rainfall induced landslides in December 2004 in south-western Umbria, central Italy: types, extent, damage and risk assessment, Nat. Hazards Earth Syst. Sci., 6, 237–260, doi:10.5194/nhess-6-237-2006, 2006. 749

Carrara, A., Cardinali, M., Detti, R., Guzzetti, F., Pasqui, V., and Reichenbach, P.: GIS techniques and statistical models in evaluating landslide hazard, Earth Surf. Processes, 16, 427–445, doi:10.1002/esp.3290160505, 1991. 749

Cascini, L. and Versace, P.: Relationship between rainfall and landslide in a gneissic cover, in: Proceedings of the 5th International Symposium on Landslides, Lausanne, Switzerland, 10–15 July 1988, vol. 1, edited by: Bonnard, C., 565–570, 1988. 749

Catani, F., Casagli, N., Ermini, L., Righini, G., and Menduni, G.: Landslide hazard and risk mapping at catchment scale in the Arno River basin, Landslides, 2, 329–342, doi:10.1007/s10346-005-0021-0, 2005. 749

Corominas, J. and Moya, J.: Reconstructing recent landslide activity in relation to rainfall in the Llobregat River basin, Eastern Pyrenees, Spain, Geomorphology, 30, 79–93, available at: http://www.sciencedirect.com/science/article/B6V93-3YS8JHH-8/2/58792b4a7097ce611f0586788e2c2a9f, 1999. 749

Corominas, J. and Moya, J.: A review of assessing landslide frequency for hazard zoning purposes, Eng. Geol., 102, 193–213, doi:10.1016/j.enggeo.2008.03.018, special issue: Landslide Susceptibility, Hazard and Risk Zoning for Land Use Planning, available at: http://www.sciencedirect.com/science/article/pii/S0013795208001841, last access: 21 March 2013, 2008. 748

Crosta, G.: Regionalization of rainfall thresholds: an aid to landslide hazard evaluation, Environ. Geol., 35, 131–145, doi:10.1007/s002540050300, 1998. 749

Crosta, G. B. and Dal Negro, P.: Observations and modelling of soil slip-debris flow initiation processes in pyroclastic deposits: the Sarno 1998 event, Nat. Hazards Earth Syst. Sci., 3, 53–69, doi:10.5194/nhess-3-53-2003, 2003. 749

Crosta, G. B. and Frattini, P.: Distributed modelling of shallow landslides triggered by intense rainfall, Nat. Hazards Earth Syst. Sci., 3, 81–93, doi:10.5194/nhess-3-81-2003, 2003. 749

Crozier, M.: Multiple-occurrence regional landslide events in New Zealand: hazard management issues, Landslides, 2, 247–256, doi:10.1007/s10346-005-0019-7, 2005. 749

Crozier, M. J.: Prediction of rainfall-triggered landslides: a test of the Antecedent Water Status Model, Earth Surf. Processes, 24, 825–833, doi:10.1002/(SICI)1096-9837(199908)24:9<825::AID-ESP14>3.0.CO;2-M, 1999. 749

Crozier, M. J., Eyles, R. J., Marx, S. L., McConchie, J. A., and Owen, R. C.: Distribution of landslips in the Wairarapa hill country, New Zeal. J. Geol. Geop., 23, 575–586, doi:10.1080/00288306.1980.10424129, 1980. 749

Dai, F., Lee, C., and Ngai, Y.: Landslide risk assessment and management: an overview, Eng. Geol., 64, 65–87, doi:10.1016/S0013-7952(01)00093-X, 2002. 754

De Vita, P., Reichenbach, P., Bathurst, J. C., Borga, M., Crosta, G., Crozier, M., Glade, T., Guzzetti, F., Hansen, A., and Wasowski, J.: Rainfall-triggered landslides: a reference list, Environ. Geol., 35, 219–233, doi:10.1007/s002540050308, 1998. 749

D'Odorico, P., Fagherazzi, S., and Rigon, R.: Potential for landsliding: dependence on hyetograph characteristics, J. Geophys. Res.-Earth, 110, n/a–n/a, F01007, doi:10.1029/2004JF000127, 2005. 763, 764

Fell, R., Ho, K. K. S., Lacasse, S., and Leroi, E.: A framework for landslide risk assessment and management, in: Landslide Risk Management, edited by: Hungr, O., Fell, R., Couture, R., and Eberhardt, E., Taylor & Francis Group, London, 3–26, 2005. 754

Foresti, L. and Pozdnoukhov, A.: Exploration of alpine orographic precipitation patterns with radar image processing and clustering techniques, Meteorol. Appl., 407–419, doi:10.1002/met.272, 2011. 752

Foresti, L., Kanevski, M., and Pozdnoukhov, A.: Kernel-based mapping of orographic rainfall enhancement in the Swiss Alps as detected by weather radar, IEEE T. Geosci. Remote, 50, 2954–2967, 2012. 752

Gabella, M., Bolliger, M., Germann, U., and Perona, G.: Large sample evaluation of cumulative rainfall amounts in the Alps using a network of three radars, Atmos. Res., 77, 256–268, 2005. 755

Galli, M. and Guzzetti, F.: Landslide vulnerability criteria: a case study from umbria, central Italy, Environ. Manage., 40, 649–665, doi:10.1007/s00267-006-0325-4, 2007. 759

Germann, U., Galli, G., Boscacci, M., and Bolliger, M.: Radar precipitation measurement in mountainous region, Q. J. Roy. Meteor. Soc., 132, 1669–1692, 2006. 755

Germann, U., Berenguer, M., Sempere-Torres, D., and Zappa, M.: REAL – ensemble radar precipitation estimation for hydrology in mountainous region, Q. J. Roy. Meteor. Soc., 135, 445–456, 2009. 764

Ghosh, S., van Westen, C. J., Carranza, E. J. M., and Jetten, V. G.: Integrating spatial, temporal, and magnitude probabilities for medium-scale landslide risk analysis in Darjeeling Himalayas, India, Landslides, 9, 371–384, doi:10.1007/s10346-011-0304-6, 2012. 749

Glade, T.: Establishing the frequency and magnitude of landslide-triggering rainstorm events in New Zealand, Environ. Geol., 35, 160–174, doi:10.1007/s002540050302, 1998. 749

Glade, T., Crozier, M., and Smith, P.: Applying probability determination to refine landslide-triggering rainfall thresholds using an empirical “Antecedent Daily Rainfall Model”, Pure Appl. Geophys., 157, 1059–1079, doi:10.1007/s000240050017, 2000. 749

Godt, J., Baum, R., Savage, W., Salciarini, D., Schulz, W., and Harp, E.: Transient deterministic shallow landslide modeling: Requirements for susceptibility and hazard assessments in a GIS framework, Eng. Geol., 102, 214–226, doi:10.1016/j.enggeo.2008.03.019, 2008. 749

Greco, R., Giorgio, M., Capparelli, G., and Versace, P.: Early warning of rainfall-induced landslides based on empirical mobility function predictor, Eng. Geol., 153, 67–79, doi:10.1016/j.enggeo.2012.11.009, 2013. 749

Gullà, G., Antronico, L., Iaquinta, P., and Terranova, O.: Susceptibility and triggering scenarios at a regional scale for shallow landslides, Geomorphology, 99, 39–58, doi:10.1016/j.geomorph.2007.10.005, 2008. 749

Guzzetti, F., Peruccacci, S., Rossi, M., and Stark, C.: The rainfall intensity–duration control of shallow landslides and debris flows: an update, Landslides, 5, 3–17, doi:10.1007/s10346-007-0112-1, 2008. 749

Hilker, N., Aller, D., and Hegg, C.: Ereignisanalyse Hochwasser 2005: Teil 1 – Prozesse, Schäden und erste Einordnung, chap. Schäden, Bundesamt für Umwelt BAFU, edited by: Bezzola, G. R. and Hegg, C., Eidg. Forschungsanstalt WSL, Bern and Birmensdorf, Switzerland, 127–148, 2007 (in German). 750, 753

Hilker, N., Badoux, A., and Hegg, C.: The Swiss flood and landslide damage database 1972–2007, Nat. Hazards Earth Syst. Sci., 9, 913–925, doi:10.5194/nhess-9-913-2009, 2009. 753

Iida, T.: A stochastic hydro-geomorphological model for shallow landsliding due to rainstorm, Catena, 34, 293–313, available at: http://www.sciencedirect.com/science/article/B6VCG-3VTYVWW-5/1/272affa188fa14bbfd4d7290700da4c3, last access: 21 March 2013, 1999. 763

Iida, T.: Theoretical research on the relationship between return period of rainfall and shallow landslides, Hydrol. Process., 18, 739–756, doi:10.1002/hyp.1264, 2004. 763

Jaboyedoff, M. and Bonnard, C.: Report on landslide impacts and practices in Switzerland: Need for new risk assessment strategies, in: The 2007 International Forum on Landslide Disaster Management, edited by: Ho, K. and Li, V., Geotechnical Division, The Hong Kong Institution of Engineers, Hong Kong, 79–97, 2007. 750, 766

Jaiswal, P., van Westen, C. J., and Jetten, V.: Quantitative estimation of landslide risk from rapid debris slides on natural slopes in the Nilgiri hills, India, Nat. Hazards Earth Syst. Sci., 11, 1723–1743, doi:10.5194/nhess-11-1723-2011, 2011. 749

Kanevski, M., Pozdnoukhov, A., and Timonin, V.: Machine Learning for Spatial Environmental Data: Theory, Applications and Software, EPFL Press, Lausanne, Switzerland, 2009. 756

Matsushi, Y. and Matsukura, Y.: Rainfall thresholds for shallow landsliding derived from pressure-head monitoring: cases with permeable and impermeable bedrocks in Boso Peninsula, Japan, Earth Surf. Processes, 32, 1308–1322, doi:10.1002/esp.1491, 2007. 749

Merz, B., Kreibich, H., Thieken, A., and Schmidtke, R.: Estimation uncertainty of direct monetary flood damage to buildings, Nat. Hazards Earth Syst. Sci., 4, 153–163, doi:10.5194/nhess-4-153-2004, 2004. 760

Michoud, C., Derron, M.-H., Jaboyedoff, M., Nadim, F., and Leroi, E.: Classification of landslide-inducing anthropogenic activities, in: 5th Canadian Conference on Geotechnique and Natural Hazards, 15–17 May 2011, Kelowna, BC, Canada, 10 pp., 2011. 766

Montgomery, D. and Dietrich, W.: A physically based model for the topographic control on shallow landsliding, Water Resour. Res., 30, 1153–1171, 1994. 749

Mueller, R. and Loew, S.: Predisposition and cause of the catastrophic landslides of August 2005 in Brienz (Switzerland), Swiss J. Geosci., 102, 331–344, doi:10.1007/s00015-009-1315-3, 2009. 753

Nguyen, H., Wiatr, T., Fernández-Steeger, T., Reicherter, K., Rodrigues, D., and Azzam, R.: Landslide hazard and cascading effects following the extreme rainfall event on Madeira Island (February 2010), Nat. Hazards, 65, 635–652, 2013. 749

Pack, R., Tarboton, D. G., and Goodwin, C. N.: The SINMAP approach to terrain stability mapping, in: 8th Congress of the International Association of Engineering Geology, 21–25 September 1998, Vancouver, British Columbia, Canada, 8 pp., 1998. 749

Preuth, T., Glade, T., and Demoulin, A.: Stability analysis of a human-influenced landslide in eastern Belgium, Geomorphology, 120, 38–47, doi:10.1016/j.geomorph.2009.09.013, 2010. 767

Raetzo, H. and Rickli, C.: Ereignisanalyse Hochwasser 2005: Teil 1 – Prozesse, Schäden und erste Einordnung, chap. Rutschungen, edited by: Bezzola, G. R. and Hegg, C., Bundesamt für Umwelt BAFU, Eidg. Forschungsanstalt WSL, Bern and Birmensdorf, Switzerland, 195–210, 2007 (in German). 750, 752, 753, 776, 777

Remondo, J., Bonachea, J., and Cendrero, A.: A statistical approach to landslide risk modelling at basin scale: from landslide susceptibility to quantitative risk assessment, Landslides, 2, 321–328, doi:10.1007/s10346-005-0016-x, 2005. 749

Rickli, C., Raetzo, H., McArdell, B., and Presler, J.: Ereignisanalyse Hochwasser 2005: Teil 2 – Analyse von Prozessen, Massnahmen und Gefahrengrundlagen, chap. Hanginstabilitäten, edited by: Bezzola, G. R. and Hegg, C., Bundesamt für Umwelt BAFU, Eidg. Forschungsanstalt WSL, Bern and Birmensdorf, Switzerland, 97–116, 2008 (in German). 750, 753, 756

Rotach, M., Appenzeller, C., and Albisser, P. E.: Starkniederschlagsereignis August 2005, Arbeitsberichte 211, MeteoSchweiz, Zürich, Switzerland, 2006 (in German). 751, 752

Seed, A. W., Srikanthan, R., and Menabde, M.: A space and time model for design storm rainfall, J. Geophys. Res.-Atmos., 104, 31623–31630, doi:10.1029/1999JD900767, 1999. 763

Sideris, I., Gabella, M., Erdin, R., and Germann, U.: Real-time radar-raingauge merging using spatiotemporal co-kriging with external drift in the alpine terrain of Switzerland, Q. J. Roy. Meteor. Soc., in review, 2013. 755, 756

Tarolli, P., Borga, M., Chang, K.-T., and Chiang, S.-H.: Modeling shallow landsliding susceptibility by incorporating heavy rainfall statistical properties, Geomorphology, 133, 199–211, doi:10.1016/j.geomorph.2011.02.033, 2011. 763

Trümpy, R.: Geology of Switzerland, Part A: An outline of the Geology of Switzerland, Wepf & Co. Verlag, Basel, Switzerland, 1980. 751

University of Bern and FOWG: Geological Map of Switzerland 1 : 500 000, Swisstopo, Bern, Switzerland, ISBN 3-906723-39-9, 2005a. 751

University of Bern and FOWG: Tectonic Map of Switzerland 1 : 500 000, Swisstopo, Bern, Switzerland, ISBN 3-906723-56-9, 2005b. 751

Valley, B., Thuro, K., Eberhardt, E., and Raetzo, H.: Geological and geotechnical investigation of a shallow translational slide along a weathered rock/soil contact for the purpose of model development and hazard assessment, in: Proceedings of the 9th International Symposium on Landslides, Rio de Janeiro, 28 June–2 July 2004, edited by: Lacerda, W. A., Ehrlich, M., Fontoura, S. A. B., and Sayão, A. S. F., A. A. Balkema, 385–391, 2004. 766

van Westen, C., van Asch, T., and Soeters, R.: Landslide hazard and risk zonation – why is it still so difficult?, B. Eng. Geol. Environ., 65, 167–184, doi:10.1007/s10064-005-0023-0, 2006. 748

von Ruette, J., Papritz, A., Lehmann, P., Rickli, C., and Or, D.: Spatial statistical modeling of shallow landslides – validating predictions for different landslide inventories and rainfall events, Geomorphology, 133, 11–22, doi:10.1016/j.geomorph.2011.06.010, 2011. 753

Whittaker, K. A. and McShane, D.: Comparison of slope instability screening tools following a large storm event and application to forest management and policy, Geomorphology, 145–146, 115–122, doi:10.1016/j.geomorph.2012.01.001, 2012. 749

Wieczorek, G. F.: Landslide triggering mechanisms, in: Landslides Investigation and Mitigation, edited by: Turner, A. K. and Schuster, R. L., Special Report 247, Transportation Research Board, National Research Council, National Academy Press, Washington, DC, 76–90, 1996. 749

WSL: Swiss flood and landslide damage database, http://www.wsl.ch/fe/gebirgshydrologie/HEX/projekte/schadendatenbank/index_EN, last access: 26.02.2013, 2012. 753

Wüest, M., Frei, C., Altenhoff, A., Hagen, M., Litschi, M., and Schär, C.: A gridded hourly precipitation dataset for Switzerland using rain-gauge analysis and radar-based disaggregation, Int. J. Climatol., 30, 1764–1775, 2010. 764

Yu, F.-C., Chen, T.-C., Lin, M.-L., Chen, C.-Y., and Yu, W.-H.: Landslides and rainfall characteristics analysis in Taipei City during the Typhoon Nari event, Nat. Hazards, 37, 153–167, doi:10.1007/s11069-005-4661-0, 2006. 749

Table 1. Fitted parameters of the gamma distribution.

Precipitation [mm]	LF α	LF β	FLMC α	FLMC β	MM α	MM β
114–134	0.0323	1.4438	0.1347	0.7346	0.0683	1.0392
134–158	0.3604	0.5403	0.2241	0.9303	0.0801	2.6114
158–184	0.1927	0.9673	0.1288	2.1937	0.1531	4.3495
184–219	0.0839	3.7578	0.2026	2.7379	0.2265	6.0948
219–321	0.1214	7.0373	0.2457	5.4336	0.4966	4.4464

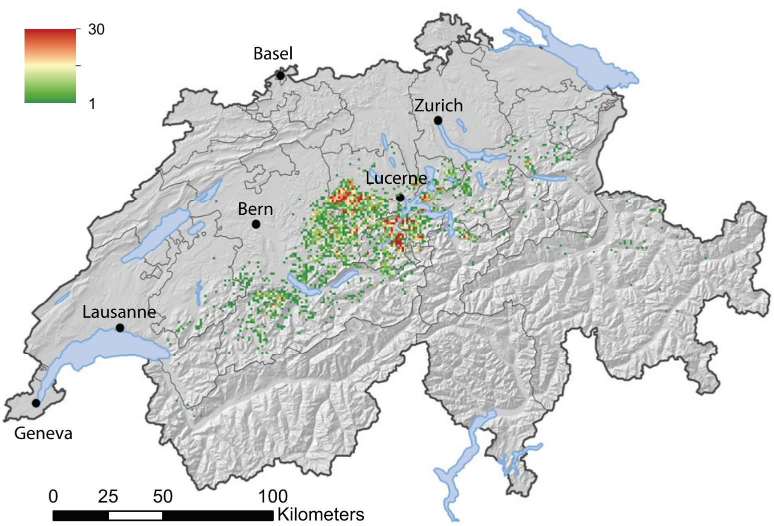

Fig. 1. Number of landslides in 1 km^2 cells (after Raetzo and Rickli, 2007, hillshade: © Swisstopo).

Discussion Paper | Discussion Paper | Discussion Paper | Discussion Paper |

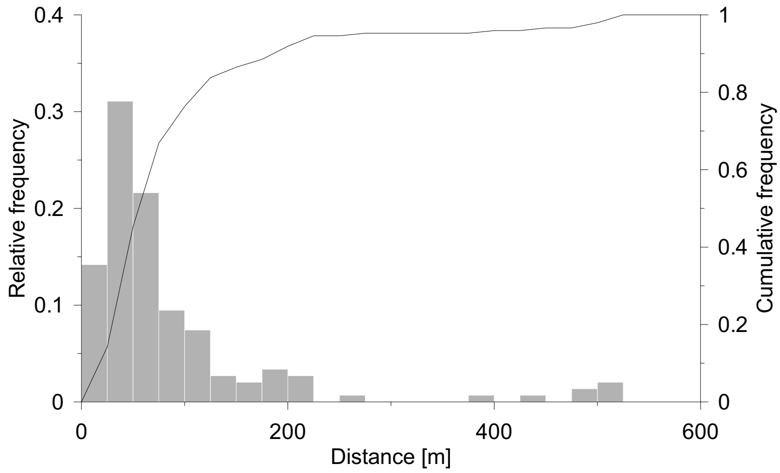

Fig. 2. Relative and cumulative frequency of the distance traveled by 148 landslides (Raetzo and Rickli, 2007).

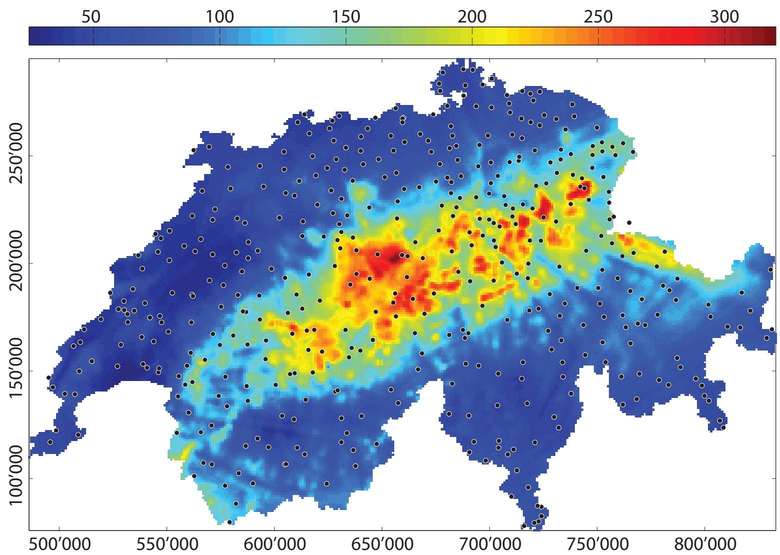

Fig. 3. Total rainfall accumulation from 18 to 23 August 2005 [mm] estimated by MLP. Dots represent the stations used for the interpolation.

Discussion Paper | Discussion Paper | Discussion Paper | Discussion Paper |

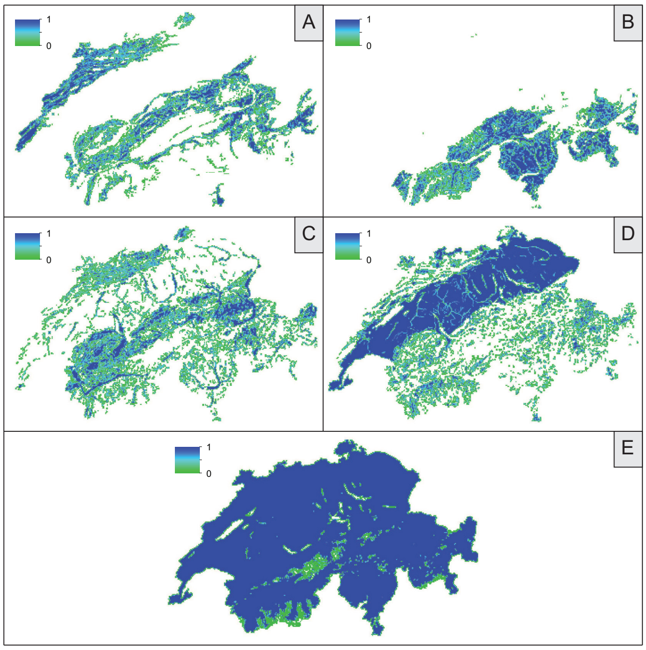

Fig. 4. Probabilistic lithological maps showing the proportion of each lithological unit. Values range from green (lithological group sligthly present) to blue, whereas white means that the lithological group is non-existent in the cell; **(A)** Limestone Formations (LF); **(B)** Cristalline Formations (CF), **(C)** Flysch, Loose material (except moraine), Marls and Claystones (FLMC), **(D)** Molasse and Moraine (MM) and **(E)** total. In map **(E)**, white tones mark the absence of lithological formations (i.e. lakes, glaciers) and other countries, while green tones depict their partial presence within the model cell, which occurs when the cumulative proportion of the 4 units is below 1.

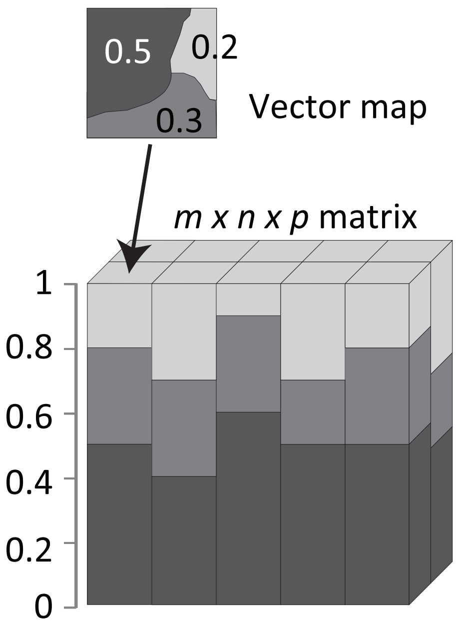

Fig. 5. Schematic transformation of the geotechnical map into a $m \times n \times p$ matrix which gives for each cell the lithological units cumulative distribution. A lithology is assigned at each model iteration by choosing a random number u. For example, if $u = 0.6$ in the lower left cell, since $0.5 < u < 0.8$, the second geology is assigned.

Discussion Paper | Discussion Paper | Discussion Paper | Discussion Paper |

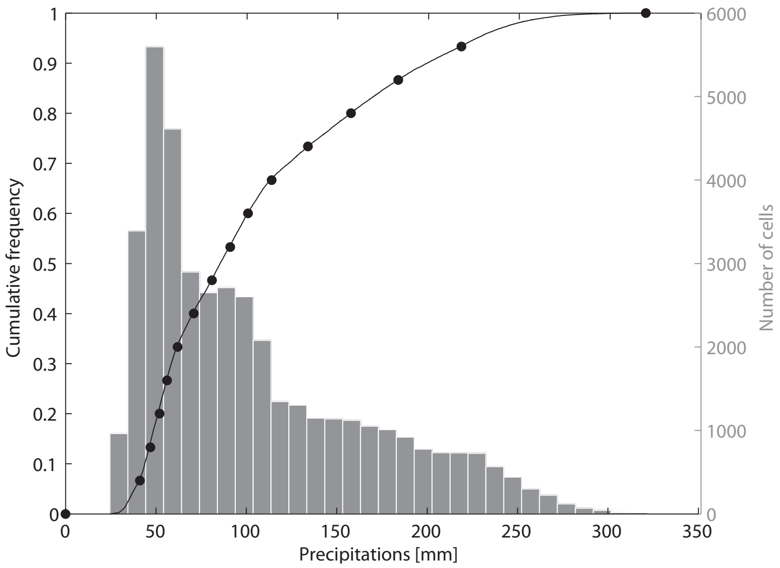

Fig. 6. Cumulative distribution of the spatial precipitation amounts. Dots show the class limits and are rounded to the upper value.

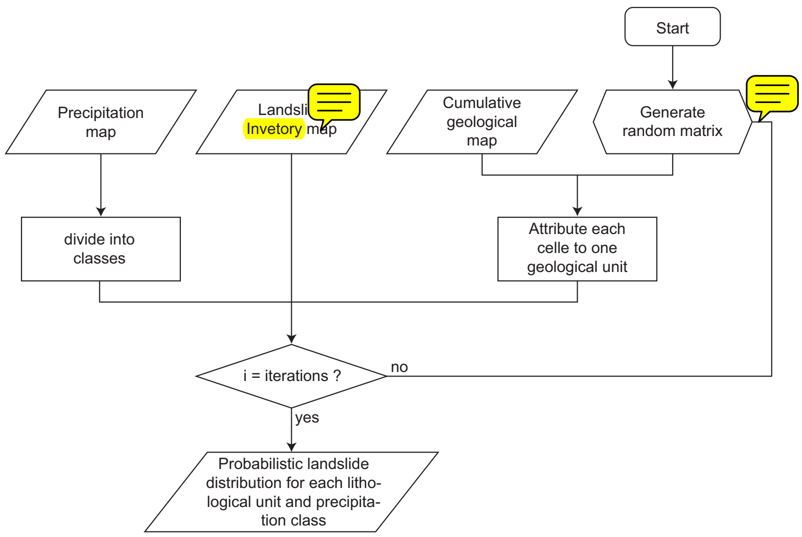

Fig. 7. Flow diagram showing the assessment methodology used to obtain the cumulative frequency of landslide number per lithological unit and precipitation class.

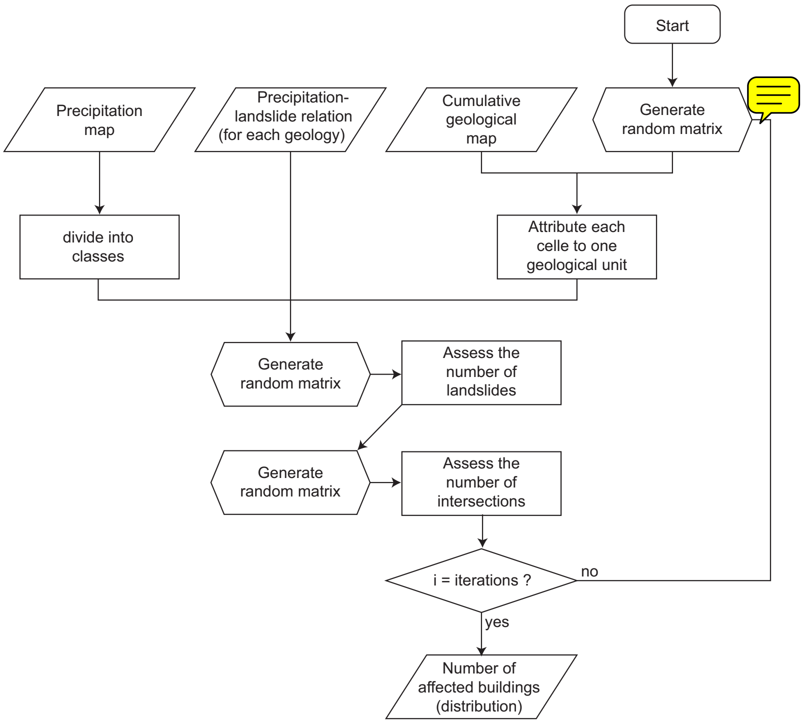

Fig. 8. Flow diagram showing the assessment methodology used to obtain the number of affected buildings.

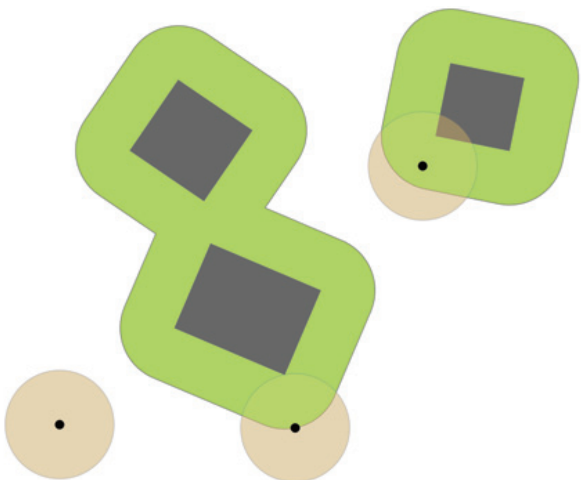

Fig. 9. Schematic example of intersection probability. The houses (in grey) are expanded with a buffer (in green). Thus, if the center of a circular landslide (in brown), with a radius equal to the buffer distance, occurs inside of the buildings + buffer area, the landslide is assumed to reach a house. The probability of intersection is then given by the ratio of the buildings + buffer area with the total area. In this example, the probability that a landslide, knowing it occurs, reaches a house is 0.158. The buffer permits to simplify the intersection probability calculation since landslides can then be considered as points, without however neglecting their surface. The intersection probability of a point and a surface is indeed easier to calculate than the intersection probability of two shapes.

Discussion Paper | Discussion Paper | Discussion Paper | Discussion Paper |

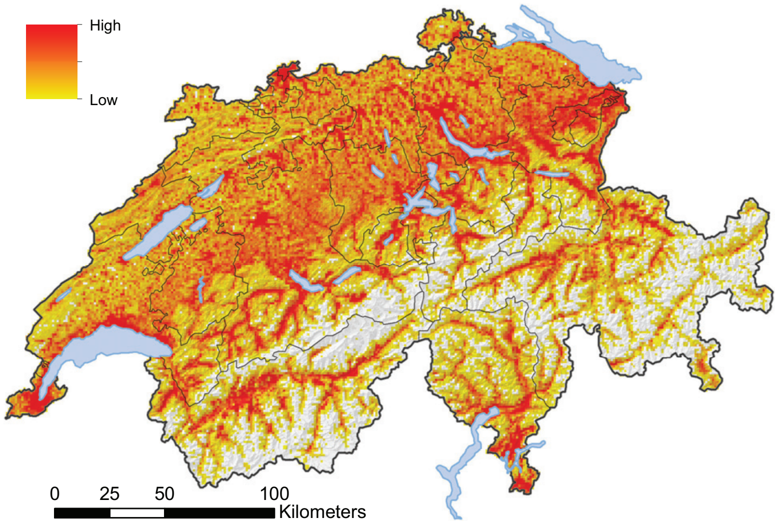

Fig. 10. Intersection probability map displaying the conditional probability for a 100 m radius circular landslide to affect a house for each cell of the model. High means that the probability is equal or close to one, yellow that it is close to 0, whereas white indicate a null probability (hillshade: © Swisstopo).

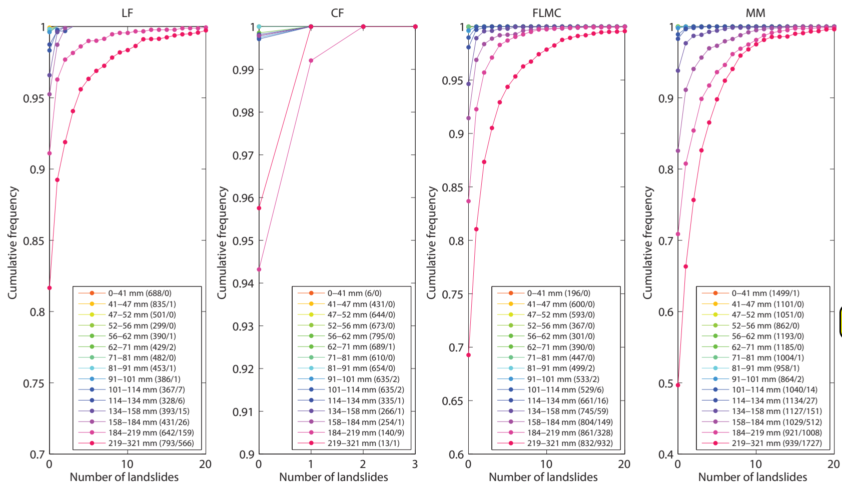

Fig. 11. Landslide relation with precipitation and lithological group. The curves for small precipitation amounts are not visible because of the low number of landslides. Note that scales are not similar. Numbers between brackets are respectively the number of cells in the class and the number of landslides in the cells, averaged over the iterations.

Discussion Paper | Discussion Paper | Discussion Paper | Discussion Paper |

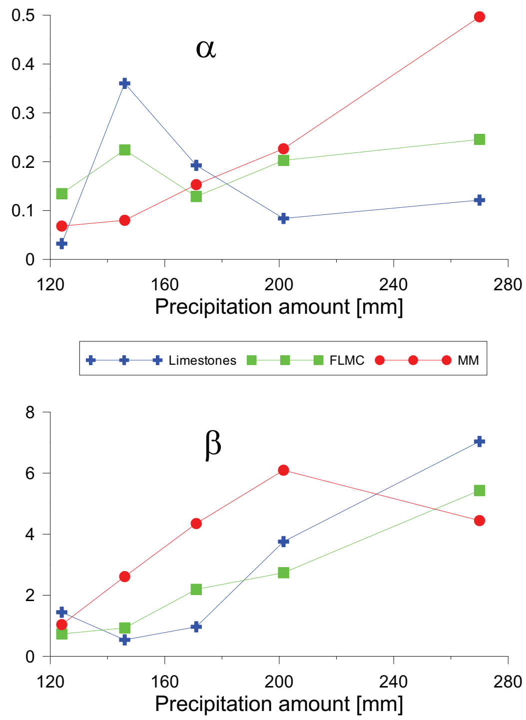

Fig. 12. Fitted parameters for α and β of the gamma distribution.

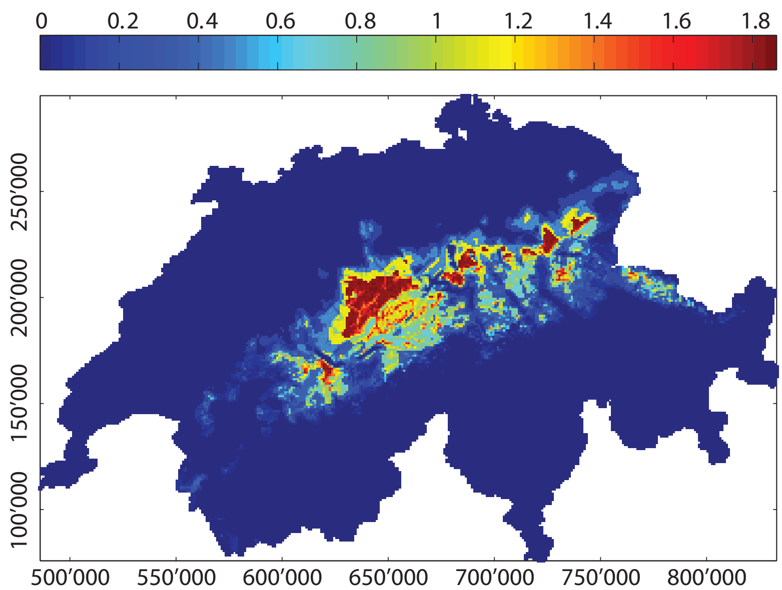

Fig. 13. Mean modeled number of landslides with the gamma functions. X- and Y-labels are the Swiss Easting and Swiss Northing coordinates [km].

Discussion Paper | Discussion Paper | Discussion Paper | Discussion Paper |

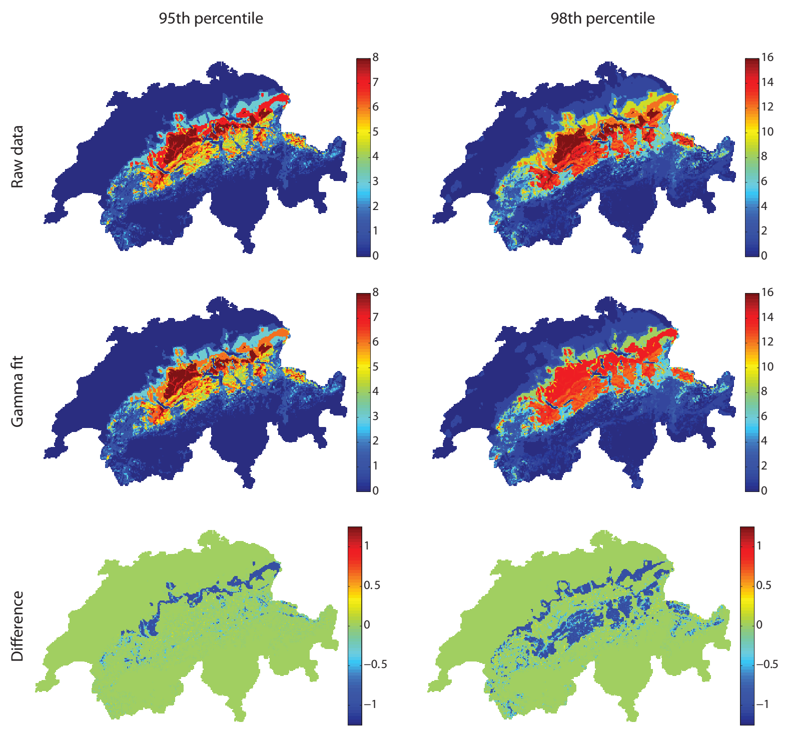

Fig. 14. 95th and 98th percentiles of the number of landslides using raw data (first row) and gamma fits (second row). The third presents the difference between the raw and gamma fits of both percentiles.

Discussion Paper | Discussion Paper | Discussion Paper | Discussion Paper |

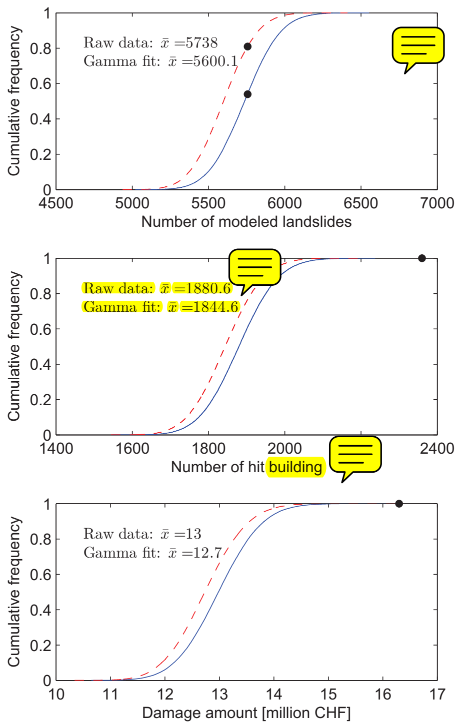

Fig. 15. Number of landslides, number of hit buildings and damage amount calculated from raw data (blue solid line) and gamma fits (red dashed line). Mean value $\bar{x}$ for each line is displayed on the graph, whereas black dots correspond to the data of the event or the expected number of affected buildings.

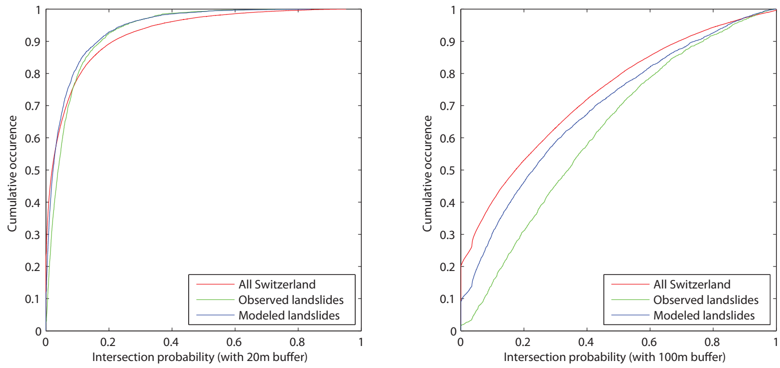

Fig. 16. Comparison of the intersection probability for the cells in which landslides occurred and in which landslides have been modeled (cells with a mean above 0.5 have been kept). As a comparison, the distribution over all Switzerland is shown.